European Journal of Radiology 69 (2009) 43–49

Contents lists available at ScienceDirect

European Journal of Radiology

journal homepage: www.elsevier.com/locate/ejrad

Dynamic optical breast imaging: A novel technique to detect and characterize tumor vessels

Laure S. Fournier[a,b,*], Daniel Vanel[c], Alexandra Athanasiou[c], Wolfgang Gatzemeier[d], I.V. Masuykov[e], Anwar R. Padhani[f], Clarisse Dromain[c], Ken Galetti[d], Robert Sigal[c], Alberto Costa[f], Corinne Balleyguier[c]

[a] Université Paris Descartes, Hôpital Européen Georges Pompidou, Radiology Department, 20 rue Leblanc, 75015 Paris, France
[b] University Paris Descartes, Faculté de Médecine, EA4062, Laboratoire de Recherche en Imagerie, site Necker, 156 rue de Vaugirard, 75015 Paris, France
[c] Institut Gustave-Roussy, Radiology Department, 39 rue Camille Desmoulins, 94805 Villejuif, France
[d] Division of Breast Surgery, Fondazione Salvatore Maugeri, Pavia, Italy
[e] DOBI Medical International Inc, Mahwah, NJ, USA
[f] Paul Strickland Scanner Centre, Mount Vernon Hospital, Northwood, UK

ARTICLE INFO

Article history:
Received 23 July 2008
Accepted 28 July 2008

Keywords:
Optical imaging
Breast cancer
Breast tumors
Diagnostic imaging
Dynamic imaging

ABSTRACT

Purpose: To prospectively determine the diagnostic accuracy of optical absorption imaging in patients with Breast Imaging Reporting and Data System (BI-RADS) 3–5 breast lesions.
Materials and methods: Forty-six patients with BI-RADS classification 3 (11%), 4 (44%) or 5 (44%) lesions, underwent a novel optical imaging examination using red light to illuminate the breast. Pressure was applied on the breast, and time-dependent curves of light absorption were recorded. Curves that consistently increased or decreased over time were classified as suspicious for malignancy. All patients underwent a core or surgical biopsy.
Results: Optical mammography showed a statistical difference in numbers of suspect pixels between benign ($N=12$) and malignant ($N=35$) lesions (respectively 1325 vs. 3170, $P=0.002$). In this population, optical imaging had a sensitivity of 74%, specificity of 92%, and diagnostic accuracy of 79%. The optical signal did not vary according to any other parameter including breast size or density, age, hormonal status or histological type of lesions.
Conclusion: Optical imaging is a low-cost, non-invasive technique, yielding physiological information dependent on breast blood volume and oxygenation. It appears to have a good potential for discriminating benign from malignant lesions. Further studies are warranted to define its potential role in breast cancer imaging.

1. Introduction

Breast cancer is the most frequent cancer in women [1]. Its incidence is estimated worldwide to be approximately 37.4/100,000 (1/2670 women), though in developed countries the incidence is higher, estimated at 103.7/100,000 (1/960). It is also the cause of the highest mortality rate related to cancer for women, estimated to be 13.3/100,000 (1/7500) worldwide, or 30.9/100,000 (1/3240) in developed countries. Current investigation of breast cancer is performed by X-ray mammography, sometimes supplemented by ultrasound and/or magnetic resonance imaging (MRI). Key limitations of conventional imaging relate to diagnostic accuracy; they all benefit from a satisfactory sensitivity, but a poor specificity. Faced with millions of women between 50 and 75 years old being screened for breast cancer, it is essential to accurately characterize breast anomalies detected with these techniques, to avoid missing a cancer (false negative), but also to avoid biopsy or surgery on a benign mass (false positive). Studies indicate that between 2/3 and 4/5 of breast biopsies reveal lesions to be benign [2]. Moreover, mammography used as a primary or a problem-solving tool exposes patients to ionizing radiation.

The use of light for breast cancer diagnosis dates back to the 1920s, when transillumination was used to investigate breast cancer [3], but low sensitivity and specificity limited its clinical usefulness. With progress in photonic technologies, mathematic modeling of light propagation through tissues, and increased knowledge of the photophysical properties of tissues, optical imaging has evolved to a state where a re-evaluation of its use is warranted.

The purpose of this prospective study was to prospectively determine the diagnostic accuracy of near-infrared breast optical absorption imaging with breast compression in patients with

* Corresponding author at: Université Paris Descartes, Hôpital Européen Georges Pompidou, Radiology Department, 20 rue Leblanc, 75015 Paris, France.
E-mail address: laure.fournier@gmail.com (L.S. Fournier).

0720-048X/$ – see front matter © 2008 Elsevier Ireland Ltd. All rights reserved.
doi:10.1016/j.ejrad.2008.07.038

Breast Imaging Reporting and Data System (BI-RADS) 3–5 classification lesions, using pathology as a reference.

2. Materials and methods

2.1. Patients

2.1.1. Informed consent

The study was conducted between March 2003 and January 2004 at two institutions. The study was approved by the local ethics committees of the two institutions and was performed in accordance with the current version of the Declaration of Helsinki and the International Conference on Harmonization of Good Clinical Practice Guidelines. Informed consent was obtained from all patients after the nature of the examinations was explained fully.

2.1.2. Inclusion criteria

Inclusion criteria included women over 18 years old in whom a planned biopsy or surgery for a suspect lesion that was diagnosed at mammography and/or ultrasound as a BI-RADS grade 3 ("probably benign (i.e. uncertain) finding"), 4 ("suspicious abnormality") or 5 ("highly suggestive of malignancy") lesion [2], and the capability of giving informed consent.

2.1.3. Exclusion criteria

The following exclusion criteria were applied: patients who did not have all relevant records available for review at the investigational site; patients who were biopsied at another site; patients who had a core or excisional biopsy of the ipsilateral breast within the past 3 months; patients who had surgical clips or scarring from a prior biopsy of the ipsilateral breast; patients who had implants; patients who had piercings on the breast.

2.2. Reference imaging

Patients underwent an X-ray mammography including at least two views: cranial-caudal and oblique, and if necessary lateral views, compression views or magnifications. Some patients also underwent an ultrasound examination. Results of mammography

Fig. 1. The ComfortScan optical mammography system. The patient stands upright and her breast is placed in the breast holder. The entire procedure takes less than 10 min.

and ultrasound were scored in a standardized way, using the BI-RADS classification [2], independent of optical imaging results.

2.3. Optical imaging

2.3.1. Image acquisition

Dynamic optical breast imaging (DOBI) was performed on the same day as the biopsy. The ComfortScan (DOBI Medical International, Inc., Mahwah, NJ, USA) is a novel optical mammography imaging system (Fig. 1). The details of the technique are described in a previous publication [4]. During the examination, the patient stood in front of the machine while her breast was positioned (cranial-caudal) onto a panel of 127 light-emitting diodes (LED) mounted on an illuminator plate inclined 30° from horizontal plane that supported the breast from below. The breast was maintained between the tray containing the LED and a thin silicone membrane that acted as a breast holder. The LED illuminated the breast of the patient with a far-red laser light wavelength (640 nm). Light was transmitted through the breast and quantified on the other side by a low-noise charge coupled device (CCD) camera.

The illumination did not always cover the totality of the breast. The operator positioned the patient's breast on the support tray and selected reference LED that illuminated the region of the breast containing the suspicious area (lateral, central or medial, and anterior or posterior), as determined by prior mammography. Two pointers were placed on the nipple and on the supposed localization of the lesion in the software operating the machine. The soft transparent membrane in contact with the upper surface of the breast was then inflated under computer control and exerted a gentle, uniform pressure on the breast. The pressure was set to 5 mmHg for the first 15 s of the scan, raised to 10 mmHg over the next 30 s (the dynamic image sequence), and lowered back to 5 mmHg for the final 15 s. Forty-five frames were acquired overall (five baseline before applying pressure and 40 during the dynamic sequence). Transmitted light was detected by the CCD throughout the scan and recorded by the computer. The entire acquisition sequence took 1 min.

2.3.2. Image processing

The image data were processed to generate dynamic images of the superior and inferior portions of the breast in a cranial-caudal view, combined to the medial and lateral portions according to the position of the nipple marker. Four zones were therefore defined: 'superior lateral', 'superior medial', 'inferior lateral' and 'inferior medial'. The dynamic image sequence was represented by $I(x, y, t)$, where 'x' and 'y' represent each spatial point and 't' represents time in seconds. A reference frame, Iref, was memorized after the first illumination cycle following the onset of the first 5 mmHg pressure step (breast shape had stabilized). The dynamic signature (DS) at each spatial point (x, y) was then calculated as follows:

$$DS(x, y, t) = (I(x, y, t) - Iref)/Iref.$$

The images were displayed in color scale to reveal time-dependent changes in the transmitted light intensity caused by the pressure change. The following standard filter rules applied to

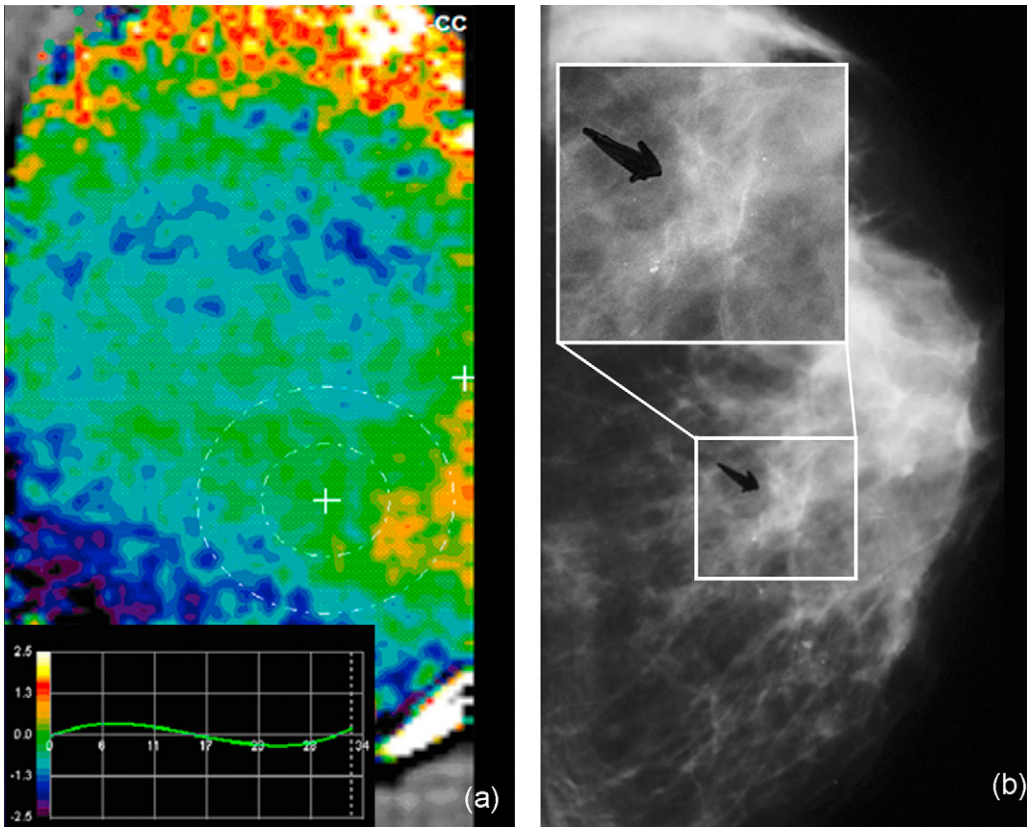

Fig. 2. Optical image (a) and corresponding cranio-caudal mammography view (b) of 58-year-old patient. The red (or white) pixels in the optical image represent pixels with a temporal absorption curve suspect of malignancy. Green pixels are pixels that are not suspect (no significant light attenuation). The pointer on the right of the optical image shows the location of the nipple on the image. The pointer surrounded by two circles is where the lesion was located on the mammogram. Both pointers were placed by the radiologist during the acquisition. Mammography showed a 1-mm cluster of pleomorphic calcifications in the medial region of the breast (a blow-up is inserted), coded BI-RADS 4 by the institution's radiologists. Optical imaging yielded very few red suspect pixels in the region of the abnormality. The red pixels observed on the sides of the breast were interpreted as due to border artifacts. A pixel was selected on the image as an example of a non-suspect pixel, coded in green, yielding a time-curve of optical signal (bottom of the image). This curve, though oscillating, is grossly stable over time. Pathology diagnosed a benign lesion, namely fibrocystic disease.

the optical images acquired: number of saturated pixels >20; light intensity (detected by the CCD camera) <400 units; illuminated area to breast area ratio ≤25%. The image processing software classified the temporal curves for each image pixel in two categories: consistently increasing or decreasing intensity over time displayed in red, considered as suspect for malignancy; and sinusoidal or absence of variation of intensity over time displayed in green. The results were displayed as a parametric image (Figs. 2 and 3).

The images were quantitatively and qualitatively analyzed by LSF and DV who were blinded to the results of pathology. Both readers working in consensus evaluated the imaging data noting the number of suspect pixels and total pixels evaluated. A category of malignant or non-malignant was assigned according to curve shape and confluence of red pixels at the site of the suspected lesion.

2.4. Pathologic findings

All lesions underwent a core (under stereotaxic or sonographic guidance) or excisional biopsy. They were fixed in 10% formalin, embedded in paraffin, and sectioned. Hematoxylin–eosin staining was performed. Pathologists categorized the tumors as benign or malignant and specified the histological type. The pathologists were also blinded to the results of optical imaging.

2.5. Statistical analysis

All quantitative data were displayed as means ± standard deviations. Group differences between benign and malignant lesions, but also according to menopausal status, breast size or breast density, with respect to values of number of suspect pixels were compared using an ANOVA test (Statview 5.0.1, SAS Institute Inc., Cary, NC, USA). A P value <0.05 was considered significant. A correlation analysis was performed to seek a correlation between age of patients or size of lesion on mammography and optical imaging numbers of suspect pixels. A Receiver Operator Characteristic (ROC) curve was established (MedCalc 7.6.0.0, Mariakerke, Belgium) to evaluate the performance as a diagnostic test of DOBI optical mammography.

3. Results

3.1. Selection of cases

A total of 78 data sets in 71 patients with the ComfortScan system were collected from March 2003 to January 2004.

Patients who had insufficient or saturated illumination of the breast, or a focal reference illumination not matching the area of interest indicated by the mammography or sonography reports were excluded from the analysis (N = 30). This meant that the suspect region of the breast had not been correctly illuminated.

After application of these criteria, the database returned 48 datasets. Of these data, one patient had incomplete clinical records (missing mammography report). A total of 47 datasets were available for interpretation and analysis.

3.2. Clinical and mammography findings

Forty-six women (median age 59 years old, age range 28–79 years) underwent near-infrared optical mammography imaging of the breast, 15 women (33%) were pre-menopausal, and 31 (67%) were menopausal (hormonal status was not recorded for one patient). Forty-seven breasts were imaged (one patient having bilateral anomalies on mammography). In total, 47 lesions were identified on mammography and explored by core or surgical biopsy.

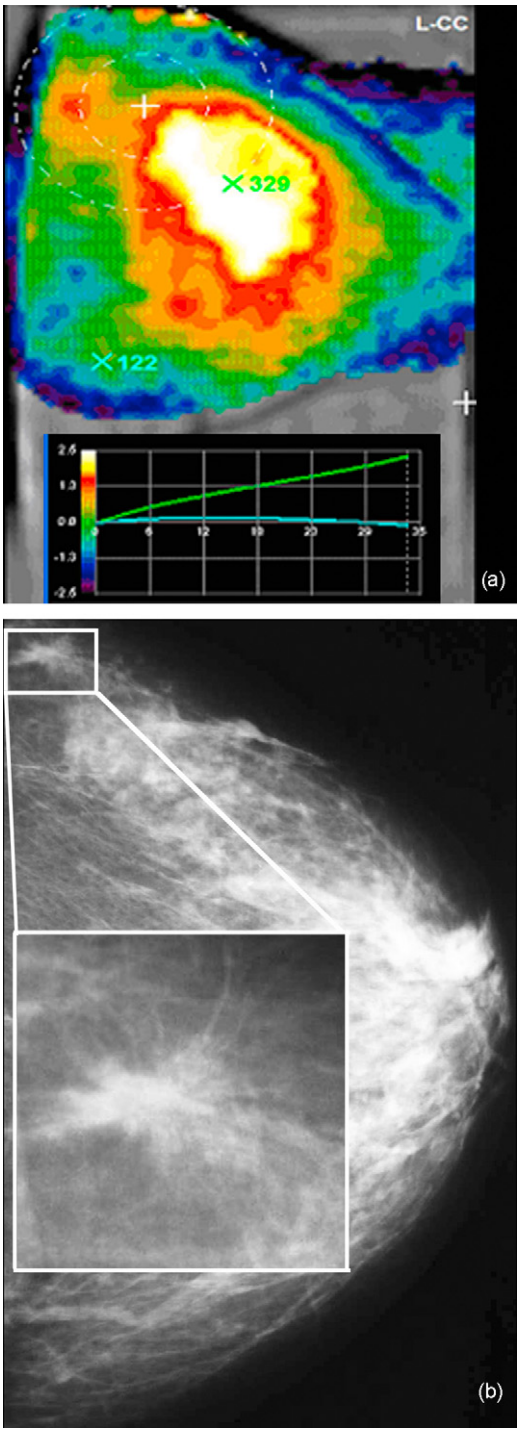

Fig. 3. Optical image (a) and corresponding cranio-caudal mammography view (b) of 59-year-old patient. The red (or white) pixels in the optical image represent pixels with a temporal absorption curve suspect of malignancy. Green pixels are pixels that are not suspect (no significant light attenuation). The pointer on the right of the optical image shows the location of the nipple on the image. The pointer surrounded by two circles is where the lesion was located on the mammogram. Both pointers were placed by the radiologist during the acquisition. A spiculated 10-mm density was visible on mammography, in the lateral region of the cranial-caudal view. Inserted is a blow-up of the lesion, which was interpreted as a BI-RADS 5 lesion by the institution's radiologists. Optical imaging revealed a large zone of red pixels, signaling numerous suspect pixels. A suspect pixel was selected on the image (green pointer, optical signal intensity measured at 329), yielding a time-curve of optical signal (bottom of the image). This curve constantly increases over time. Another pixel was selected in a non-suspect region (light blue pointer, optical signal intensity measured at 122). Its curve is flat. Pathology diagnosed a malignant lesion (intraductal carcinoma).

Breast size of patients was also recorded, according to measure of breast cups. Three (7%) women had A-sized breasts, 22 (49%) had B-sized breasts, 14 (31%) had C-sized breasts and 6 (13%) had D-sized breasts. In one case, breast size was not included in the case report forms.

Breast density was classified (according to BI-RADS) as 1 for 4 women (9%), 2 for 27 women (59%), and 3 for 15 women (32%). Breast density was not recorded for two women.

Twenty-three (49%) lesions were in the right breast, 24 (51%) in the left breast.

Thirty-one lesions (67%) appeared as nodules or masses on mammography, 7 (15%) as isolated microcalcifications, 7 (15%) as focal asymmetric densities, 1 (2%) as an architectural distortion, and one was not described in the reports. A majority of the lesions were localized in the superior lateral quadrant (15/47, 32%).

Five (11%) lesions were classified BI-RADS 3 according to the BI-RADS classification, 20 (44%) were classified BI-RADS 4, and 20 (44%) were classified BI-RADS 5. The mammography reports did not mention the BI-RADS classification for two lesions. Lesion size was estimated on mammography, mean was calculated to be 15 ± 9 mm (ranging from 1 to 50 mm). Lesions were non-palpable, apart from two of them.

3.3. Pathological findings

Twelve lesions (26%) were diagnosed as benign and 35 (74%) as malignant. Among the 12 benign lesions, 6 (50%) were fibrocystic disease, 3 (25%) were fibroadenomas, 2 (17%) were normal fibrofatty tissue, and 1 (8%) was a papilloma. Among the 35 malignant lesions, 20 (57%) were intraductal carcinoma, 11 (31%) were intralobular carcinoma, and 1 (3%) was a papillary carcinoma. Three (9%) malignant lesion types were not further classified (malignant, not otherwise classified).

3.4. Optical imaging (Figs. 2 and 3)

No adverse effects were observed during or after optical mammography acquisition. On the contrary, every woman stated that it was a short examination, without discomfort (particularly compared to mammography).

3.5. Statistical analysis

Mean scores for the number of suspect pixels were respectively for all benign and malignant tumors 1325 ± 984 vs. 3170 ± 1881 ($P = 0.002$). Differences between optical imaging measures of benign vs. malignant lesions remained statistically significant when lesions ≤20 mm (on mammography) were considered ($N = 38$, $P = 0.004$), or lesions ≤10 mm ($N = 18$, $P = 0.02$). Fig. 4 represents the distribution of number of suspect pixels for benign and malignant lesions (≤ or >20 mm). The ROC curve (Fig. 5) showed that the optimal cut-off value for the number of pixels that were suspect according to optical imaging was 2050, yielding a sensitivity of 74%, a specificity of 92%, a positive predictive value of 93%, a negative predictive value of 55% and a diagnostic accuracy of 79%. For lesions ≤20 mm, the optimal cut-off value was also 2050, yielding a sensitivity of 72%, a specificity of 85%, a positive predictive value of 90%, a negative predictive value of 61% and a diagnostic accuracy of 76%. Table 1 represents a cross-tabulation between the results of optical imaging and pathology for all lesions and those ≤20 mm. The false positive lesion was a fibroadenoma; the nine false negatives included seven intraductal carcinomas, one intralobular carcinoma and one papillary carcinoma. They measured 1–40 mm; four appeared as nodules on mammography, four were focal asymmetric densities, and one was a cluster of microcal-

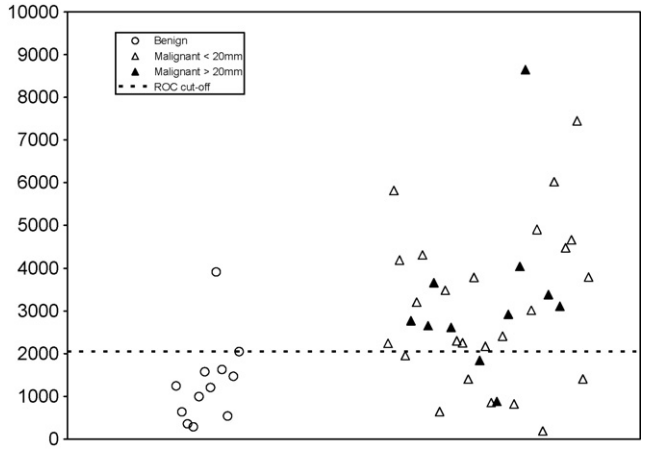

Fig. 4. Scatter plot of number of suspect pixels on optical imaging for benign and malignant lesions. Benign lesions are represented as white circles (all were ≤20 mm). Malignant lesions ≤20 mm are represented by white triangles and those >20 mm as black triangles. The dotted line represents the cut-off at 2050 determined by the ROC curve to differentiate benign from malignant lesions using this optical imaging technique.

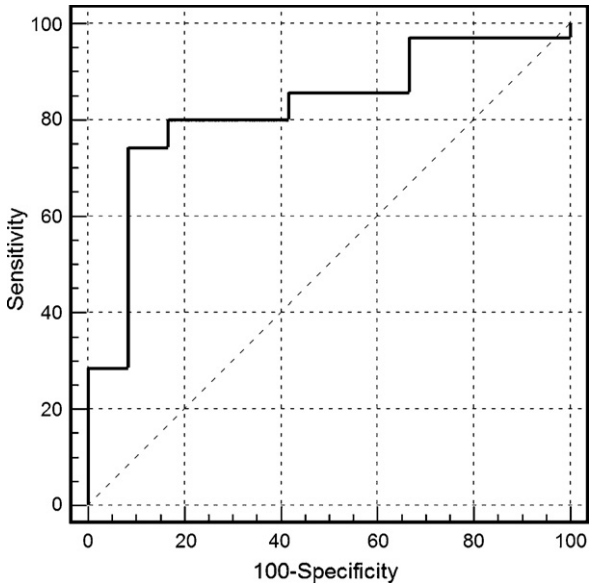

Fig. 5. Receiver Operator Characteristic (ROC) curves for near-infrared optical imaging as a diagnostic test. Sensitivity and specificity were calculated for different values of numbers of suspect pixels for all lesions. The area under the curve was calculated to be 0.82 for all lesions (and 0.81 for lesions ≤20 mm), qualifying this technique as a good diagnostic test.

Table 1
Results of optical imaging (number of pixels suspect of malignancy) compared to pathology for all lesions and for lesions ≤20 mm

	Malignant	Benign	
All lesions			
Number of pixels >2050	TP = 26	FP = 1	PPV = 96%
Number of pixels ≤2050	FN = 9	TN = 11	NPV = 55%
	Se = 74%	Sp = 92%	Total = 47
Lesions ≤20 mm			
Number of pixels > 2050	TP = 18	FP = 1	PPV = 95%
Number of pixels ≤2050	FN = 7	TN = 11	NPV = 61%
	Se = 72%	Sp = 92%	Total = 37

TN, is true negatives; TP, true positives; FN, false negatives; FP, false positives; Se, sensitivity; Sp, specificity; PPV, positive predictive value and NPV, negative predictive value.

cifications (the 40 mm lesion). All women were menopaused, and breast density was rated 2 or 3.

The multivariate ANOVA analysis showed on the contrary, no statistical difference between optical imaging measures according to patients menopausal status ($P = 0.63$), side of the lesion ($P = 0.83$), breast size ($P = 0.20$) or breast density ($P = 0.51$).

The correlation analysis showed no correlation between optical measure of number of pixels suspect of malignancy and age of patients ($r = -0.03$, $P = 0.83$) or size of lesion ($r = 0.19$, $P = 0.19$).

4. Discussion

A novel optical imaging instrument, measuring changes of absorption of near infrared laser light by breast tissue while applying pressure, showed statistically significant differences between benign and malignant lesions, in patients selected for the presence of abnormal mammographic findings classified 3, 4 or 5 according to the BI-RADS classification. The area under the ROC curve was calculated to be 0.82 with a standard error of 0.062, qualifying this technique as a good diagnostic test for differentiating benign from malignant breast lesions in this population [5]. These differences were not linked to patients menopausal status or age, breast size or density, or the size of lesion.

Optical imaging has numerous potential advantages, including the use of non-ionizing low energy light radiation, high sensitivity, continuous data acquisition for real-time monitoring, and low cost. It is particularly interesting for breast cancer imaging, since it concerns so many women worldwide. Moreover, it does not have the setback of mammography which uses ionizing radiation and is uncomfortable because of the need to apply compression, or the high cost of MRI.

The absorption of near-infrared laser light (600–900 nm) within breast tissue is primarily related to the presence of hemoglobin, where deoxy-hemoglobin is more attenuating than oxy-hemoglobin [6,7]. In a breast cancer, the process of angiogenesis leads to an increased blood volume in the tumor. Neoangiogenic tumor vessels have an abnormal vasculature, they are tortuous and hyperpermeable [8]. A disparity between oxygen demand and supply leads to tumor hypoxia and an increase in the deoxyhemoglobin content of blood [9]. By applying external pressure on the breast while imaging, it is thought that blood is transiently trapped within tumor vessels which will result in a rapid decrease in local blood oxygenation, leading to an increase in deoxyhemoglobin concentration. This increase in deoxyhemoglobin concentration further increases absorption of near-infrared light. Thus, the application of external pressure while imaging increases the sensitivity of the DOBI method compared to simple infrared absorption imaging.

To our knowledge, this is the first study performed on a large number of patients comparing results of mammography and dynamic optical absorption imaging.

It is important to state that almost all lesions were non-palpable, and that this diagnostic test had high sensitivities and specificities even for small lesions under 20 mm, for which detection and characterization benefits most the patients.

This approach was purely quantitative and automated, therefore not subject to wide intra- or inter-observer variations, which make mammography for example, a difficult discipline to learn [10,11].

One of the limitations usually brought up for optical imaging is that large breasts might be too thick to be imaged using light. In our study, 20 patients were excluded because their data did not fit the filter criteria described in Section 3. Four patients (20%) were a size E cup. However, there were also size B ($N = 6$, 30%), size C ($N = 7$, 35%), and size D ($N = 3$, 15%) breasts that were excluded also according to the same criteria suggesting that breast size was not an important limiting feature. Also, breast density did not seem to be an issue, since structures that are opaque to X-rays (fibrous tissue) are transparent to near-infrared optical imaging (collagen, for example, absorbs in the blue spectrum [12].

This study is a preliminary study designed to evaluate near infrared optical mammography's potential in breast imaging, and presents some limitations.

A large number of examinations (30/78, 38%) were excluded secondarily for technical reasons. These were mostly the first patients imaged in each center with is technique. This demonstrates that there is a learning curve to acquire images, ad as the technicians' and radiologists' experience increased, there were practically no more technical failures.

In this study, we chose to image women with BI-RADS 3, 4 or 5 lesions because these lesions were due to be biopsied providing histological analysis. There is therefore a bias since only women with mammographic abnormalities were studied. Further studies will be necessary to define optical aspects of normal breasts.

However, the population studied was comparable to others reported in the literature including BI-RADS 3, 4 or 5 lesions. For BI-RADS 4 lesions, 55% (11/20) were malignant, and for BI-RADS 5 lesions, 95% (19/20) were malignant. These results are comparable to other results found in the literature [2,13]. Also, most of our patients (67%) were post-menopausal, and their lesions were mostly malignant (81%, 26/32, vs. 60%, 9/15 for pre-menopausal women). Interestingly, we had a greater number of lobular carcinoma (25%, 11/35 of malignant lesions), whereas it is usually much less represented compared to intraductal carcinoma [14–16].

Nine cancers were not detected with this technique. They were not the smallest lesions, nor were they situated in the largest or most dense breasts. Six had been classified BI-RADS 5 by mammography, therefore correctly described as most certainly malignant lesions. These results imply that mammography and optical imaging will probably be complementary, as they describe different physiological properties of tissues.

Finally, it is important to note that infrared light scatters in biological tissues resulting in a large area of light attenuation. This scattering effect can result in a poor concordance between lesion location on mammography and on DOBI imaging. Instead, it is the geometric relationship of the illuminating diode, lesion and CCD camera that determines the location of the abnormality on the optical images. Therefore, this functional imaging technique cannot be used to locate a lesion. As a result, we cannot be certain that each IR abnormality visualized in our study does indeed correspond to the lesion described on mammography.

We have used a novel imaging instrument that combines infrared imaging with light breast compression in women with equivocal or suspect mammographic abnormalities and have shown that it has potential in distinguishing benign from malignant lesions. This is an early evaluation of this technique which relies on physiological properties of breast tissue to impart optical contrast on images. Further evaluation will be required to optimize the technique, evaluate its sensitivity and specificity in a wider range of patients, and explore its potential role in patient management.

Acknowledgment

L.S.F. has been supported by a post-doctoral stipend from the Association pour la Recherche sur le Cancer (2003).

References

[1] Breast Cancer Statistics: IARC GLOBOCAN 2002. (Accessed January 6, 2005, at http://www-dep.iarc.fr/).

[2] Liberman L, Menell JH. Breast imaging reporting and data system (BI-RADS). Radiol Clin North Am 2002;40:409–30.
[3] Cutler M. Transillumination as an aid in the diagnosis of breast lesions. Surg Gynecol Obstet 1929;48:721–9.
[4] Athanasiou A, Vanel D, Balleyguier C, et al. Dynamic optical breast imaging: a new technique to visualise breast vessels: comparison with breast MRI and preliminary results. Eur J Radiol 2005;54:72–9.
[5] Interpreting diagnostic tests. Tape T. University of Nebraska Medical Center. (Accessed January 17, 2005 at http://gim.unmc.edu/dxtests/Default.htm).
[6] Cerussi AE, Berger AJ, Bevilacqua F, et al. Sources of absorption and scattering contrast for near-infrared optical mammography. Acad Radiol 2001;8:211–8.
[7] Peters VG, Wyman DR, Patterson MS, Frank GL. Optical properties of normal and diseased human breast tissues in the visible and near infrared. Phys Med Biol 1990;35:1317–34.
[8] McDonald DM, Baluk P. Significance of blood vessel leakiness in cancer. Cancer Res 2002;62:5381–5.
[9] Shah N, Cerussi AE, Jakubowski D, Hsiang D, Butler J, Tromberg BJ. The role of diffuse optical spectroscopy in the clinical management of breast cancer. Dis Markers 2003;19:95–105.
[10] Baker JA, Kornguth PJ, Floyd Jr CE. Breast imaging reporting and data system standardized mammography lexicon: observer variability in lesion description. AJR Am J Roentgenol 1996;166:773–8.
[11] D'Orsi C. The American College of Radiology mammography lexicon: an initial attempt to standardize terminology. Am J Roentgenol 1996;166:779–80.
[12] Shah N, Cerussi A, Eker C, et al. Noninvasive functional optical spectroscopy of human breast tissue. Proc Natl Acad Sci USA 2001;98:4420–5.
[13] Orel SG, Kay N, Reynolds C, Sullivan DC. BI-RADS categorization as a predictor of malignancy. Radiology 1999;211:845–50.
[14] Berg W, Gutierrez L, NessAiver M, et al. Diagnostic accuracy of mammography, clinical examination, US, and MR imaging in preoperative assessment of breast cancer. Radiology 2004;233:830–49.
[15] Helvie MA, Paramagul C, Oberman HA, Adler DD. Invasive lobular carcinoma. Imaging features and clinical detection. Invest Radiol 1993;28:202–7.
[16] Hilleren DJ, Andersson IT, Lindholm K, Linnell FS. Invasive lobular carcinoma: mammographic findings in a 10-year experience. Radiology 1991;178:149–54.